

Electric Field Characteristics of Ending Box-Air (EB-A) Type Outdoor Termination under Switching Impulse Superimposed on DC Voltage

Ik-Soo Kwon, Kuniaki Sakamoto, Jae-Hong Koo, Byeong-Cheol Mun, Sung-Won Ahn, Dong-Uk Kim and Bang-Wook Lee

Abstract— The development of Ending Box-Air (EB-A) type outdoor termination for DC environment, is presumed to have technical obstacles such as insulation material, electric field concentration, temperature rise, and space charge accumulation. In this work, we focused on the electric field concentration considering the influence of the switching impulse superimposed on pre-stressed DC voltage. Particularly, the influx of switching impulses during DC steady-state operation is a very serious condition because it could lead to a sudden change in the potential difference and an abrupt increase in the electric field intensity. Therefore, DC field analysis on EB-A type outdoor termination model was performed to understand electric field characteristics when the switching impulse is superimposed on DC voltage. A change in the electric field distribution in EB-A with the polarity and peak voltage of superimposed switching impulse was analyzed. In addition, two measurement lines were selected to verify main factors that determine the total electric field intensity under switching impulse superimposed on DC voltage. And the field intensities according to simulation cases were compared in each measurement line. Consequently, different electric fields were distributed according to polarity and peak voltage of the superimposed switching impulse on each field measurement line. In the first measurement line, a total electric field at switching impulse superposition with the opposite polarity having the largest electric potential difference was the most concentrated. On the other hand, in the second measurement line, a total field intensity was highest when the switching impulse of the same polarity as the dc voltage were superimposed. These noticeable results could be explained by the direction and magnitude of the two electric fields.

Keywords: Electric field distribution, Electric field intensity, Ending Box-Air (EB-A), Superposition, Switching impulse

I. INTRODUCTION

THE DC grid formation not only facilitates power transmission between countries and continents, but also brings economic advantages such as transmission loss reduction and efficient load management. In order to construct the DC grid, long-distance power transmission should be implemented by use of overhead and underground transmission line. And the connection of overhead and underground transmission line can be achieved by use of the Ending Box-Air (EB-A) type outdoor

termination.

EB-A type outdoor termination installed at outdoor substations are important cable accessories for connecting underground cables and overhead transmission lines. The outdoor termination of the AC transmission system has already been developed and is widely used. On the other hand, development of outdoor termination of the DC transmission system has been introduced only in some countries such as China and Japan, and the development status and core technology have not been fully reported. Also, unlike traditional insulation design techniques applied to AC outdoor termination, insulation failures were frequently occurred in DC outdoor termination due to a lack of reliable DC insulation design technology [1]. Therefore, research on DC insulation design technology should be deeply carried out to develop a reliable DC outdoor termination. In order to ensure improved insulation techniques for DC outdoor termination, an influx of the switching impulse during DC steady-state operation should be considered. Because it could cause a sudden increase in electrical stress and a very large potential difference for several tens of microseconds. In addition, it also causes insulation breakdown, which can be a cause of failure in the DC cable system [2].

In this paper, electric field analysis of EB-A under DC stress and superimposed on DC voltage considering polarities and peak voltages of switching impulse were conducted. Based on simulation results, comparison analysis of electric field characteristics for both cases were conducted. Thermal characteristics and temperature conditions were considered for all cases, because the temperature gradient in the insulation materials was generated due to the heat in the conductor occurring during power transmission [3].

II. ELECTRIC FIELD CHARACTERISTICS UNDER SWITCHING IMPULSE SUPERIMPOSED ON DC VOLTAGE

The governing equations that determine the electric field distribution can be derived from (1) - (4) [4].

This work was supported by the Human Resources Program in Energy Technology of the Korea Institute of Energy Technology Evaluation and Planning (KETEP), granted financial resource from the Ministry of Trade, Industry & Energy, Republic of Korea. (No. 20154030200730). This research was supported by the Korea Electric Power Corporation (Grant number: R16XA01).

Bang-Wook Lee is with the Division of Electrical Engineering, Hanyang University, Ansan, Republic of Korea (phone: +82-31-400-5665; e-mail of

corresponding author: bangwook@hanyang.ac.kr).

Ik-Soo Kwon, Kuniaki Sakamoto and Jae-Hong Koo are with the Division of Electrical Engineering, Hanyang University, Ansan, Republic of Korea. Byeong-Cheol Mun, Sung-Won Ahn and Dong-Uk Kim are with Power Cable Division, ILJIN Electric. CO., Hwaseong, Republic of Korea.

Paper submitted to the International Conference on Power Systems Transients (IPST2017) in Seoul, Republic of Korea June 26-29, 2017

$$\text{Electrostatic electric field : } \vec{E} = -\nabla V \quad (1)$$

$$\text{Ohm's law for current density : } \vec{J} = \sigma \vec{E} \quad (2)$$

$$\text{Gauss law for space charge : } \nabla \cdot (\epsilon_0 \epsilon_r \vec{E}) = \rho \quad (3)$$

$$\text{Current continuity equation : } \nabla \cdot \vec{J} = -\frac{\partial \rho}{\partial t} \quad (4)$$

The resistive electric field (\vec{E}_{DC}) generated by DC voltage and the capacitive electric field (\vec{E}_{SI}) by switching impulse can be obtained solving the above equations. The resistive field is highly dependent on the electrical conductivities of insulation materials. In a structure composed of two or more kinds of insulation materials having different electrical conductivity, an electric field is more concentrated on the insulation material having lower electrical conductivity. Also, as the difference in electrical conductivity between insulation materials increases, the electric field intensity also increases. On the other hand, the capacitive field is determined by the permittivity, and the electric field is more concentrated on the insulation material having a relatively lower permittivity. Since the two electric fields are determined by different factors, the total electric field intensity under switching impulse superimposed on DC voltage can be expressed as (5) [5].

$$\vec{E}_{TOTAL} = \vec{E}_{DC} + \vec{E}_{SI} \quad (5)$$

\vec{E}_{DC} and \vec{E}_{SI} mean an electric field generated by DC voltage and by switching impulse, respectively. A vector addition of the \vec{E}_{DC} and \vec{E}_{SI} determines a total electric field intensity (\vec{E}_{TOTAL}) when switching impulse superimposed on DC voltage. The \vec{E}_{TOTAL} can be illustrated in Fig. 1. Fig. 1 assumes two electric fields with the same magnitude of the electric field and with an angle of α .

When α is zero, the directions of \vec{E}_{DC} and \vec{E}_{SI} are exactly same. Therefore, the \vec{E}_{TOTAL} can be calculated by a simple vector operation, adding the magnitudes of two electric fields. On the other hand, the direction of \vec{E}_{DC} and \vec{E}_{SI} are exactly opposite when α is 180 degrees. In such case, \vec{E}_{TOTAL} can be calculated by a simple arithmetic subtraction of \vec{E}_{DC} and \vec{E}_{SI} . Thus, as shown in Fig. 1, the former produces the greatest stress and the latter produces the lowest stress under all superposition situations.

When α is in the range of 0 to 90 degrees or 270 to 360 degrees, the \vec{E}_{TOTAL} has a larger value than the \vec{E}_{DC} . Conversely, when α is in the range of 90 to 270 degrees, the \vec{E}_{TOTAL} has a smaller value than the \vec{E}_{DC} . This is entirely determined by α , which is varied by the direction of electric fields when magnitudes of two electric fields are the same.

In the case of a cable, there are only two directions. One is the electric field introduces from conductor and goes out toward sheath and the other is opposite direction. Therefore, α is only 0 or 180 degrees. When the switching impulse of the same polarity is superimposed on DC voltage, i.e. α is zero, the

electric field intensity reaches to the maximum because the direction of two electric fields are exactly same. On the other hand, when the switching impulse of the opposite polarity is superimposed on DC voltage, i.e. α is 180 degrees, the electric field under pre-stressed DC voltage is canceled out by the electric field generated from the superimposed switching impulse. Thus, it could be concluded that the prediction of the electric field distribution under switching impulse superposition situation is simple in case of the cable structure.

However, EB-A has a complex structure composed of a plurality of insulation material unlike a cable structure. As a results, directions of the two electric fields, i.e. α , are different depending on positions which makes it difficult to evaluate an influence of switching impulse superposition. Therefore, in this paper, electric field analysis was performed on the EB-A type outdoor termination through a numerical approach based on the above-mentioned governing equations to verify an effect of direction of electric fields.

III. SIMULATION CONDITIONS AND GEOMETRY MODEL SET-UP

Simulations in the EB-A model were carried out using COMSOL Multiphysics. The EB-A simulation model is composed of several insulation materials such as Cross-Linked Polyethylene (XLPE), Liquid Silicon Rubber (LSR), insulating oil, and epoxy, as shown in Fig. 2. The electrical conductivity equations against temperature (T) were used for all insulation materials. Electrical conductivity equations of XLPE, LSR,

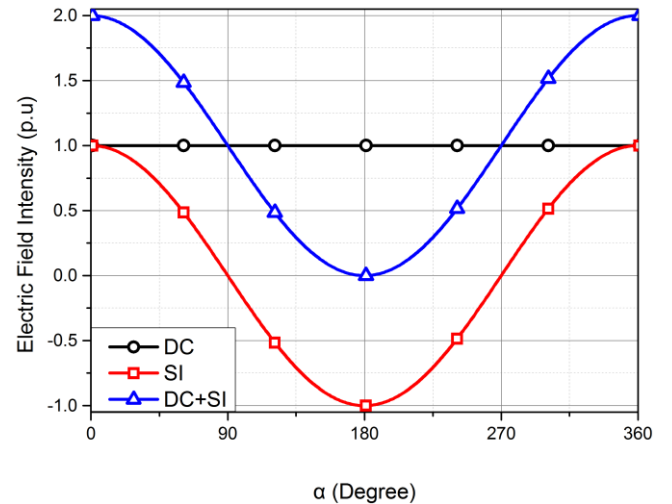


Fig. 1. Change of total electric field intensity (\vec{E}_{TOTAL}) under switching impulse superimposed on DC voltage according to α .

ML1 : Tangential Electric Field Intensity

ML2 : Normal Electric Field Intensity

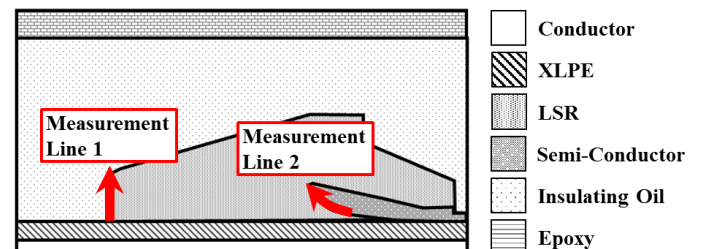


Fig. 2. EB-A simulation model geometry and measurement lines.

epoxy was obtained by a direct measurement test, and conductivity equations of insulating oil was derived by literature research [6]. A temperature gradient of 65 K between the conductor side (363.15 K) and the outermost layer (298.15 K) was reflected in all simulations.

In addition, two measurement lines were selected for comparison of electric field intensity according to location in the EB-A model. Fig. 2 shows the measurement lines of EB-A model. The purpose of measurement line 1 (ML1) is to obtain a tangential electric field intensity at the interface between LSR and insulating oil. A normal electric field intensity at the surface of semi-conductor in vicinity of a triple junction point was measured through measurement line 2 (ML2).

Fig. 3 shows the definition of superposition waveform of DC voltage and switching impulse used in simulation works. U_{DC} represents the DC rated voltage, U_{PEAK_same} and $U_{PEAK_opposite}$ that can be superimposed denote the peak values of the switching impulse from zero voltage [7]. Due to the constraints within the DC system design U_{PEAK_same} does not necessarily equal $U_{PEAK_opposite}$, i.e. the same polarity impulse is limited by surge arresters, but the opposite polarity impulse may be limited by the converter [7]. Thus, U_{SI_same} and $U_{SI_opposite}$, which mean potential differences with U_{DC} , do not need to be the same either. In this paper, electric field distributions are compared considering various U_{PEAK} and U_{SI} conditions. Regardless of the simulation cases, a switching impulse with a standard waveform of 250/2500 μ s was applied.

Table 1 shows values of U_{DC} , U_{SI} and U_{PEAK} used in simulations. The U_{DC} was fixed as 320 kV, and only polarities and peak voltages of U_{SI} and U_{PEAK} were varied. CASE 1 means a DC steady-state condition in which no switching impulse is superimposed. CASE 2 and CASE 3 are opposite in polarity only, and the magnitude of peak voltages of U_{PEAK_same} and $U_{PEAK_opposite}$ is equal to 736 kV. The magnitude of peak voltage

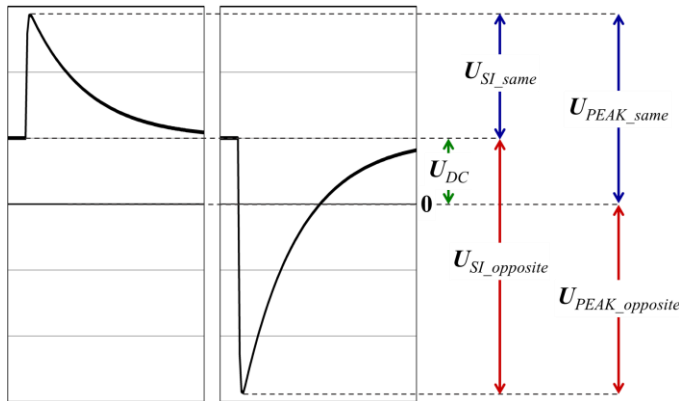


Fig. 3. Definition of superposition waveform of U_{DC} , U_{PEAK} and U_{SI} according to polarity of the switching impulse.

TABLE I
INPUT VOLTAGE VALUES IN SIMULATION

CASE No.	U_{DC} (kV)	U_{PEAK} (kV)	U_{SI} (kV)
1	+320	0	0
2	+320	+736	+416
3	+320	-736	-1056
4	+320	-96	-416

was calculated based on literature survey. One recommends to apply a test safety factor of 1.15 [8], the other specifies that a test level of switching impulse superimposed on DC voltage for the 320 kV HVDC cable systems should be no less than 2 p.u. [9]. Therefore, the U_{PEAK} were calculated as below (6):

$$U_{PEAK} = 320 \times 1.15 \times 2 = 736 \text{ [kV]} \quad (6)$$

In addition, electric field analysis was performed with CASE 4 when magnitudes of U_{SI_same} and $U_{SI_opposite}$ are identical, i.e. in case of having same potential difference (416 kV). Based on simulation results of CASE 2 and CASE 4, comparative analysis was carried out to investigate the polarity effect under the same voltage.

IV. SIMULATION RESULTS AND DISCUSSION

The distribution of \vec{E}_{TOTAL} and equipotential lines under switching impulse superimposed on pre-stressed DC voltage in the EB-A simulation model are shown in Fig. 4. A legend of the electric field is 0 to 50 kV/mm and equipotential lines are at 10% intervals from 10% to 90% of the applied maximum voltage.

Fig. 4 (a) shows the electric field distribution during DC steady-state operation, which corresponds to CASE 1. As a pure resistive electric field distribution, the electric field was highly concentrated in the LSR near triple junction point where the XLPE, LSR and semi-conductor having a relatively small volume and a lower electrical conductivity. It can be explained by the characteristic of the resistive field distribution in which the electric field intensity also increases as ratio of the electrical conductivity between the insulation materials increases [10].

Fig. 4 (b) and Fig. 4 (c) show field distributions, which correspond to CASE 2 and CASE 3, respectively. The electric field in EB-A was also distributed differently since the direction of electric field generated by switching impulses were opposite. Fig. 4 (c) and Fig. 4 (d) shows the electric field distribution of CASE 3 and CASE 4, respectively. The electric field distribution according to the magnitude of \vec{E}_{SI} under the same polarities could be investigated by comparing CASE 3 and CASE 4. In CASE 4, $U_{SI_opposite}$ was only -416 kV, while in CASE 3, $U_{SI_opposite}$ was -1056 kV, about 2.54 times higher. As the peak voltage of U_{SI} increases, the electric field becomes more influenced by the capacitive field. Therefore, the electric field was distributed similar to the capacitive field in CASE 3 which has relatively larger U_{SI} than CASE 4.

It could also be confirmed by result of electric field analysis. In case of capacitive field, the degree of the electric field concentration is relatively lower compared to resistive field because permittivity ratio is generally much lower than conductivity ratio [11]. When comparing Fig. 4 (c) and Fig. 4 (d), the degree of the electric field concentration near the triple point in Fig. 4 (d) is higher and a distortion of the equipotential lines was greater. Therefore, it could be also deduced that CASE 3 is more influenced by capacitive field.

Comparing CASE 2 and CASE 4, which has the same potential difference, electric field distributed differently since the direction of electric field generated by switching impulses

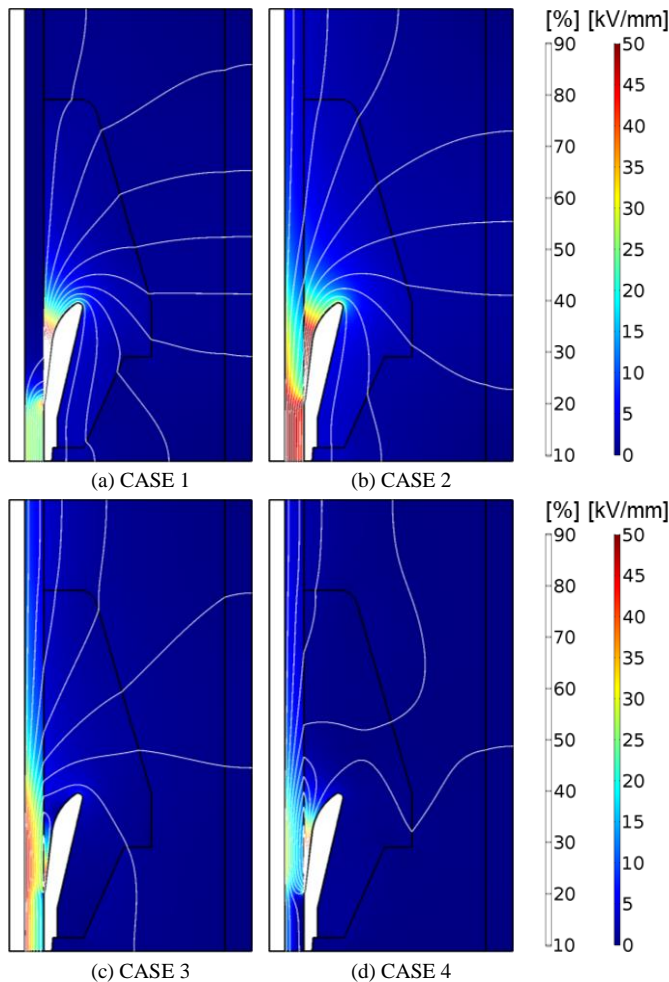


Fig. 4. The distribution of electric field (\vec{E}_{TOTAL}) and equipotential lines under switching impulse superposed on DC voltage in the EB-A model.

were opposite. Based on comparative analysis on each case, the electric field distribution is determined by the vector operation of resistive field and capacitive field. Consequently, the \vec{E}_{TOTAL} could be increased or decreased depending on α . Therefore, the electric field intensity of ML 1 and ML 2 were measured in order to verify \vec{E}_{TOTAL} according to direction of the electric field.

Fig. 5 and Fig. 6 show the magnitude and direction of the electric field intensity for each condition in ML1 and ML2. A size of the arrow indicates the intensity of the electric field, and a direction of the arrow illustrates the direction. The red and blue arrows represent the electric field during DC steady-state operation which correspond to CASE 1 and that under superimposed switching impulse of CASE 2, respectively. In addition, the black and green arrows indicate an electric field of CASE 3 and CASE 4, respectively. For electric fields generated by a switching impulse with the opposite polarity, it is clear that directions of the electric fields are completely opposite because α is 180 degrees.

In case of a tangential electric field intensity of ML1 in Fig. 5, a direction of the \vec{E}_{DC} changed depending on the position. Whereas \vec{E}_{SI} had the almost same directions. In the case of a same polarity switching impulse which correspond to CASE 2, \vec{E}_{TOTAL} decreases when the α is larger. On the other hand, in the

case of an opposite polarity switching impulse of CASE 3 and CASE 4, the higher the \vec{E}_{TOTAL} was higher as α increases.

In case of the normal electric field intensity of ML2 in Fig. 6, the α was approximately zero or 180 degrees according to polarity of switching impulse. Therefore, the electric field was the most concentrated when switching impulse having the same polarity as the DC voltage was superimposed. However, in case of switching impulse superimposed on CASE 3 and CASE 4 with the same polarity, the α is constant at 180 degrees. In this case, different electric fields are distributed depending on the magnitude of the electric field rather than the direction of the electric field. Therefore, it is expected that the electric field of CASE 3, which has a relatively larger U_{SI} , will be more concentrated than CASE 4.

In order to verify an effect of direction and magnitude, \vec{E}_{TOTAL} according to the position in each measurement lines are shown in Fig. 7 and Fig. 8. The electric field intensities were represented in p.u values based on the \vec{E}_{DC} of CASE 1.

As shown in Fig. 7, in the case of a tangential electric field intensity at ML1, the measured value differs depending on the x-axis so that different field intensities were derived. The \vec{E}_{TOTAL} of CASE 3 was the largest at x-axis coordinate range of 0~37 mm and it was about 6 times larger than the \vec{E}_{DC} . \vec{E}_{TOTAL} of CASE 2 was the largest in the range of the x-axis coordinate

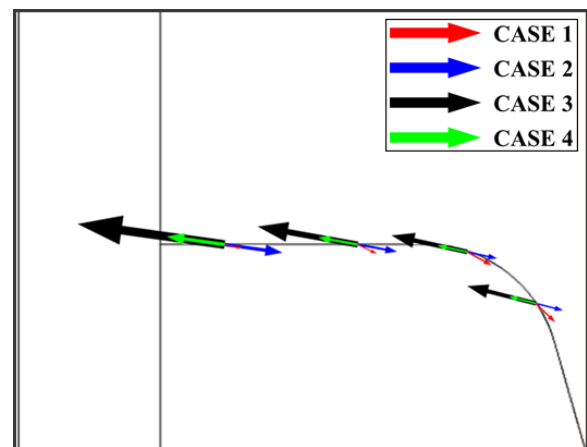


Fig. 5. Directions and magnitudes of the electric fields under switching impulse superposition according to the simulation conditions at 250 μ s at ML1.

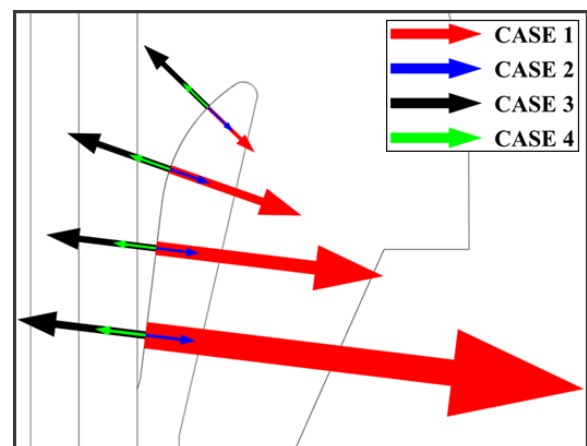


Fig. 6. Directions and magnitudes of the electric fields under switching impulse superposition according to the simulation conditions at 250 μ s at ML2.

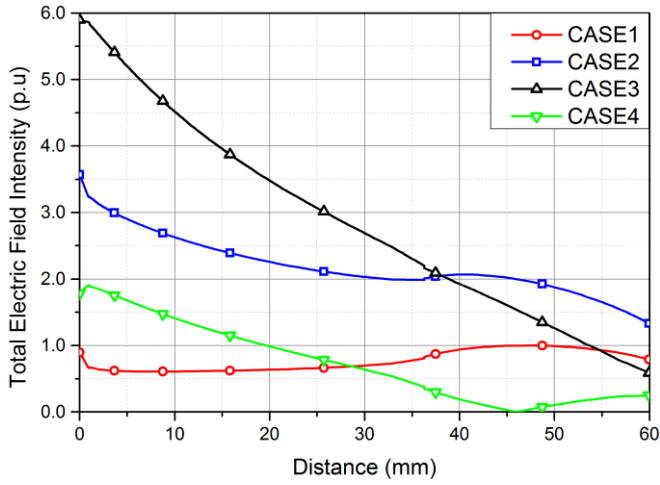


Fig. 7. Tangential electric field intensity (\vec{E}_{TOTAL}) under switching impulse superimposed on DC voltage according to the simulation conditions at 250 μ s at ML1.

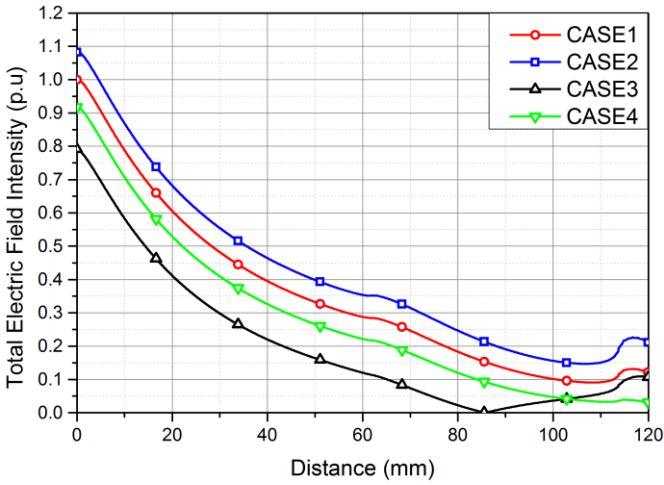


Fig. 8. Normal electric field intensity (\vec{E}_{TOTAL}) under switching impulse superimposed on DC voltage according to the simulation conditions at 250 μ s at ML2.

37~60 mm. For the range of x-axis coordinate 0~28 mm, \vec{E}_{DC} of case 1 was lowest.

The reason of the trend of \vec{E}_{TOTAL} changes according to the coordinates of the x-axis is that the factors that determine \vec{E}_{TOTAL} are different. When \vec{E}_{DC} and \vec{E}_{SI} are similar in size, α is the main determinant of \vec{E}_{TOTAL} . On the other hand, if either \vec{E}_{DC} or \vec{E}_{SI} has a significantly larger value than the other, then the electric field intensity with much larger value is a critical factor in determining \vec{E}_{TOTAL} . In comparison between CASE 3 and CASE 4, \vec{E}_{TOTAL} of CASE 3 had a larger value even though \vec{E}_{SI} was generated in the same direction because U_{SI} of the CASE 3 was larger than that of CASE 4. It means that the magnitude of electric field also affects the \vec{E}_{TOTAL} . This results could be explained by obtaining the \vec{E}_{TOTAL} of ML2.

As shown in Fig. 8, in the case of the tangential electric field intensity of ML2, α is only 0 or 180 degree. For the same polarity, \vec{E}_{TOTAL} increases because α is zero. On the other hand, in the case of the opposite polarity, since the α is 180 degree,

\vec{E}_{TOTAL} is rather reduced due to the cancellation by \vec{E}_{SI} . As a result, the electric field intensity of CASE 2 was larger than that of CASE 3 and CASE 4.

Comparing CASE 3 and CASE 4, the electric field intensity of CASE 4 was larger because \vec{E}_{SI} of CASE 3 with larger potential difference cancelled \vec{E}_{DC} more greatly. Thus, it could be concluded that \vec{E}_{TOTAL} depends on the magnitude rather than the direction if electric field when α is the same.

The field intensities of two different fields were derived from the two field measurement lines, which proved that they are influenced by both the direction and the size of the electric field. As a result, CASE 3, which has the highest electric field concentration in ML1, had the lowest field intensity in ML2.

V. CONCLUSIONS

Simulation works were performed on EB-A model to comprehend the electric field characteristics under switching impulse superimposed on DC voltage. When the switching impulse is superimposed on the DC voltage, the electric fields has shown different distribution according to the measurement lines in EB-A simulation model.

From the simulation results, it was shown that total electric field distribution composed of DC and switching impulse superposition are governed by both the direction and magnitude of the two electric fields. In a complex structure composed of composite insulation such as EB-A, an estimation of the electric field intensity according to location is not as simple as cable. It is considered that more reliable insulation design can be achieved by electric field analysis considering both the polarity and the peak value of the switching impulse which can flow in the actual cable system.

VI. REFERENCES

- [1] N. D. Jacob, and F. A. Fattal, "A practical test circuit for combined high direct voltage and switching impulse voltage multi-stress tests," in *Proc. 2016 IEEE Electrical Insulation Conference*, pp.623-626.
- [2] P. Arnold, S. Tenbohlen, W. Kohler, U. Riechert, and U. Straumann, "Fixed particles in coaxial SF 6 arrangements at various voltage stresses," in *Proc. 2014 High Voltage Engineering and Application*, pp. 1-4.
- [3] CIGRE SC D1.103: "Solid insulation in dc gas-insulated systems", CIGRE
- [4] Jeroense, Marc. "HVDC, the next generation of transmission: highlights with focus on extruded cable systems," *IEEE Transactions on Electrical and Electronic Engineering*, vol. 5, pp. 400-404, Jul. 2010.
- [5] M.J.P. Jeroense, and P.H.F. Morshuis, "Electric Field in HVDC Paper-Insulated Cables," *IEEE Trans. Dielectrics and Electrical Insulation*, vol. 5, pp. 225-236, Apr. 1998.
- [6] Nartey, E. A. "Oil/Paper Insulation for HVDC: Conductivity of Oil," 2011.
- [7] CIGRE WG B1.32: "Recommendations for testing DC extruded cable systems for power transmission at a rated voltage up to 500 kV," CIGRE Technical Brochure, No. 496, 2012.
- [8] CIGRE WG B1.42: "Recommendations for Testing DC Transition Joints for Power Transmission at a Rated Voltage Up To 500KV," CIGRE Technical Brochure, No. 622, 2015.
- [9] Wang, H., Cao, J., He, Z., Yang, J., Han, Z., and Chen, G. "Research on overvoltage for XLPE cable in a modular multilevel converter HVDC transmission system," *IEEE Trans. Power Delivery*, vol. 31, pp. 683-692, 2016.
- [10] F. H. Kreuger, *Industrial High Voltage*, vol. 3, pp. 15-22, Delft Univ. Press, 1991.
- [11] G. Mazzanti, and M. Marzinotto, *Extruded Cables for High-Voltage Direct Current Transmission*, New Jersey: Wiley, 2013.